Vibration analysis of a superconducting magnetic bearing under different temperatures

Elkin Rodriguez [a], Felipe Costa [a], Richard Stephan [a]

[a] Laboratory of Applied Superconductivity – LASUP / UFRJ, P.O.Box 68504, 21941-972 Rio de Janeiro, Brazil.
elkin@dee.ufrj.br; felipe@pee.ufrj.br; richard@dee.ufrj.br

***Abstract*—Magnetic bearings offer the best solution to mitigate mechanical friction. A variety of geometries and new materials are being studied [5][6][7][8][9]. The advantage of using a passive bearing system, like the Superconducting Magnetic Bearing (SMB), is that it offers low friction without the need of feedback control, increasing the reliability and decreasing the energy consumption. SMB devices work at very low temperatures that are often achieved with the use of liquid nitrogen inside of cryostats.**

This paper describes the design and experimental tests of a SMB passive magnetic bearing system. An innovative design of a cryostat that uses YBCO bulks refrigerated by a cryocooler is presented. With this setup, it is possible to perform vibration tests in several temperatures from 45K up to 77K to find the resonance frequency on each axis at each temperature.

Pieces of equipment that use SMB can benefit from reducing the working temperature [7][8][9]. The mechanical response of the pinning force may vary with the choice of refrigeration used.

To perform those tests, units of accelerometers are installed on the rotor body to monitor the behavior .

This improved magnetic bearing will be used in energy storage systems to reduce the instability of the rotor used in flywheel applications by changing the refrigeration temperature of the superconductor. This investigation can lead to an improvement of the levitation force, the levitation gap and damping.

I. SUPERCONDUCTING MAGNETIC BEARING

The evolution of superconductive materials and manufacturing processes allowed SMBs to withstand high strength and good radial and axial stability. This is possible with an uniform and constant temperature, since temperature variations change the behavior of the SMB. The stability and efficiency can be compromised. Such problems may be caused by environmental conditions or by the temperature control. The vacuum chamber is built to reduce the environmental influence. A bath of Liquid Nitrogen (LN_2) is normally used to temperature control of the superconducting bulk, but it has some disadvantages. For example; all pieces of equipment must be suitable for use with LN_2 and, for a safe operation, level and pressure control are needed. All this increases the cost and complexity of the system. Another technique to control the temperature is the use of a cryocooler in closed loop operation. This equipment is expensive but reduces the risk of burns with liquid nitrogen and the supply of cryogenic fluids. Energy consumption is optimized by the copper contact between the cryocooler and the superconductor.

II. PROTOTYPE

The SMB system prototype is shown schematically in Figure 1. It consists of vacuum chamber, cryocooler, internal cold plate with superconductor bulks and flywheel structure.

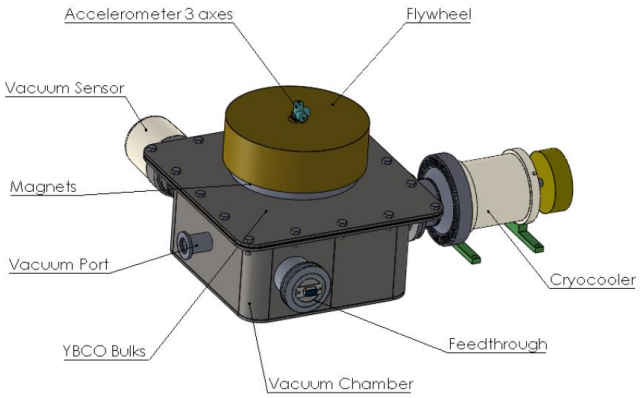

Figure 1. Figure 1. Schematic representation of the equipment with the superconductors installed inside a cryostat and cooled by a cryocooler. Sensors can be seen at the top.

A. The vacuum chamber

The vacuum chamber is a closed box constructed of stainless steel plates welded with TIG welding. It is large enough to house all internal components such as sensors, copper plate, thermal insulation and superconducting blocks and a vacuum layer to minimize heat input. It has 4 ports to: cryocooler, vacuum pump, vacuum sensor and a feedthrough for temperature sensors.

Figure 2. Photograph of the cryostat prototype.

B. *The cryocooler*

The cryocooler is a device that allows to cool down the samples in cryogenic temperatures through a Stirling cycle up to 40 K in a controlled way, using a controller unit and a Pt100 type sensor. This procedure replaces the use of liquid nitrogen and allows working temperatures lower than 77K. This model is produced by Sunpower Inc.

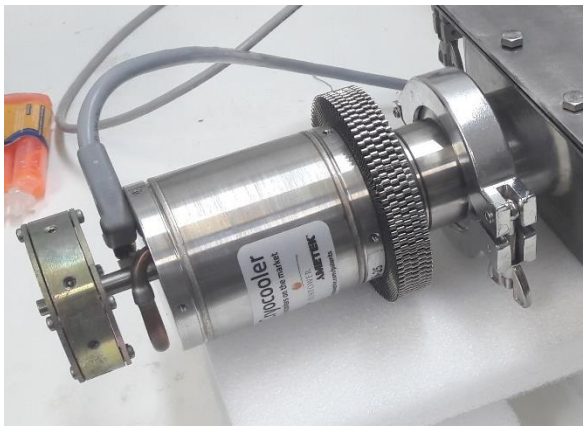

Figure 3. The equipment Cryotel MT model used.

C. *Superconductor bulks*

The YBCO blocks are installed in a copper plate to ensure good thermal conduction during the tests. In all there are 8 blocks positioned upon the board which is connected directly to the cryocooler through a thermal strap. This plate rests on thermal insulating structures to ensure the best support with minimum heat conduction input. These insulating structures are the only point of contact between the cold part and the walls of the cryostat.

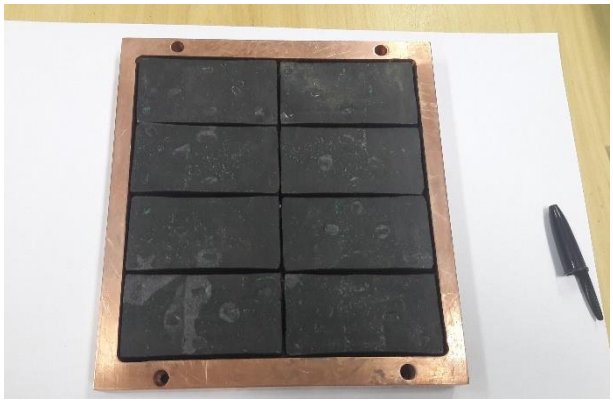

Figure 4. Copper plate with YBCO bulks before instalation.

D. *Permanent magnets*

The rotor levitating on the top of the cryostat has the shape of a disk that has Nd-Fe-B magnets arranged in a circular Halbach format. This structure has iron rings that work as magnetic flux concentrators. This part of the rotor is the one that supplies the magnetic field of the SMB. In this disk, masses can be added to change the dynamic behavior of the system with possibilities of a varied range of tests.

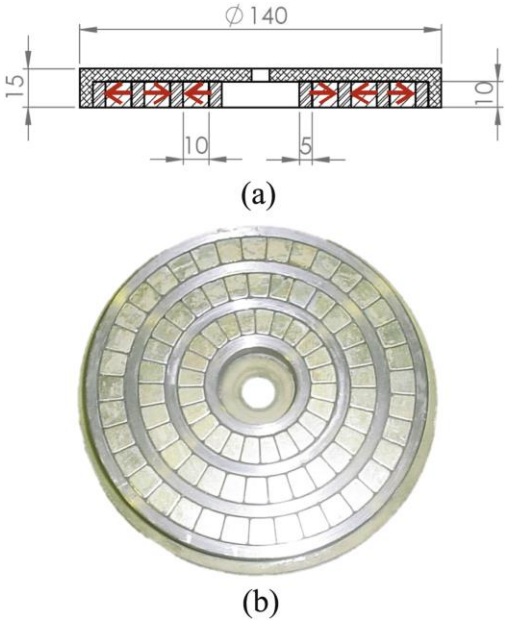

Figure 5. SMB developed: (a) dimensions of the SMB rotor in mm (the arrows indicates the magnetization); (b) photo of the SMB rotor with permanent magnets and iron rings.

E. *Temperture sensors*

Four temperature sensors are used in this arrangement. A Pt100 type sensor is used in the thermal strap near the cold head as feedback loop control. Two other Cernox (Lakeshore) sensors are used to measure the temperature of the copper plate with the superconductors and another Cernox is used to evaluate the temperature of the structures holding the cold part.

Figure 6. Temperature sensor distribution inside the cryostat.

III. METHODOLOGY

The tests performed show the temperature influence on the dynamic behavior of the SMB bearing. Some studies suggest that in high-temperature type II superconductors, such as YBCO, when at different temperatures within the mixed state and between Hc1 and Hc2, the levitation force may be different. Since the objective of the test bench is to verify the operation of a Flywheel type energy storage system with SMB bearing, an experiment was set up to verify if the resonance frequencies and the dynamic stiffness for a given rotor would also suffer variation for different temperature values below the critical temperature of the superconducting material.
The system behaves like a damped harmonic oscillator and the formulas that model this behavior are as follows:

$$\frac{d^2x}{d^2t} + 2\xi\omega_0\frac{dx}{dt} + {\omega_0}^2 x = 0 \quad (1)$$

$$\omega_0 = \sqrt{K/m} \quad (2)$$

$$\xi = \frac{c}{2\sqrt{mK}} \quad (3)$$

To this end, the experimental apparatus prepared for this test consists of a cryostat with an array of eight superconducting YBCO bulks size 36x76x14 mm mounted inside of a copper plate. This plate is cooled by a Cryotel MT cryocooler of 5W cooling power though a copper thermal strap that connect the two pieces. The entire system is connected to a Pffeifer Hi Cube 80 Pro vacuum pump to achieve a vacuum pressure of 10-6 mbar. A Mercury cryonics temperature monitoring system from Oxford instruments was also used to read the temperature of the Cernox sensors installed on the copper plate inside the cryostat.
A triaxial set of accelerometers was installed on the upper surface of the wheel of Nd-Fe-B magnets of the rotor in order to capture the attenuations and decelerations of this rotor at the time of the test. To obtain this data, a cDAQ USB chassis with NI9234 module from National Instruments was used. The collected data was processed directly on the computer through Labview software.

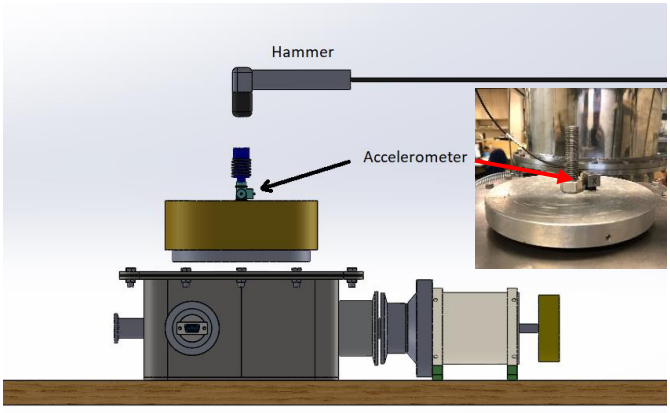

Figure 7. Experimental bench forvibration tests

Table 1. Accelerometer Specification

Triaxial Delta Tron	4525-B-001
Reference sensitivity at 159.2 Hz (X-axis)	102,6 mV/g
Reference sensitivity at 159.2 Hz (Y-axis)	99,46 mV/g
Reference sensitivity at 159.2 Hz (Z-axis)	106,0 mV/g
Measuring range	±500 ms-2

The rotor magnet disc is positioned at a height of 12mm from the cryostat stainless steel cover having 3mm thickness and a further 1 mm vacuum layer between the surface of the superconductor and the cover plate. In this way, the magnetic real gap is 16 mm between the magnets and the superconductors. This is the height of the Field Cooling of this test.

A. Procedure

The system is evacuated and the cryogenic cooler is switched on. From this moment, the magnet disk is positioned on spacers on the upper surface of the cryostat and the temperature drop is monitored to identify the desired test temperature. The tests were performed with the copper plate at temperatures of 75K, 65K and 55K, to be sure that the plate was at this temperature the minimum temperature gradient between sensors 3 and 4 was observed.

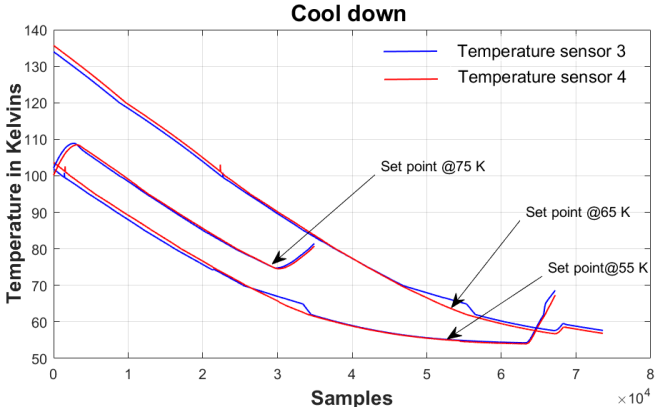

Figure 8. The cool down mesured temperatures to the test's set point

As soon as the temperature is stabilized for the test, the spacers are removed and the accelerometer is installed on the surface of the disk.
From this moment, the cryocooler is turned off so that the generated vibrations do not interfere with the test.
The force impulse is given in the direction of the Z axis downwards. The tests with the hammer are divided into 4 groups:

a) Only with the mass of the disc (1.18 kg);
b) Mass of the disc plus additional mass(1.18+2.72kg);
c) Only with the mass of the disc + flux pump
d) Mass of the disc plus additional mass + flux pump

The so-called flux pump is the procedure of moving the magnet disk in the direction of magnetic field penetration in the superconducting blocks so that the SMB bearing passes from

the largest creep flux phase and enters a more stable levitation condition.

The data of the accelerometers are acquired and processed to obtain the FFT which is realized to identify the natural frequencies at this temperature for this harmonic set.

The same procedure is done for the temperatures of 75K, 65K and 55K. After each test, at a fixed temperature, the superconducting assembly was heated until it returned to the normal state and ceased levitation to the beginning of a new test so that one test did not interfere in the next one.

B. Results and discussion

Each experiment was performed 3 times for each condition and in each test 2 impulse were given.

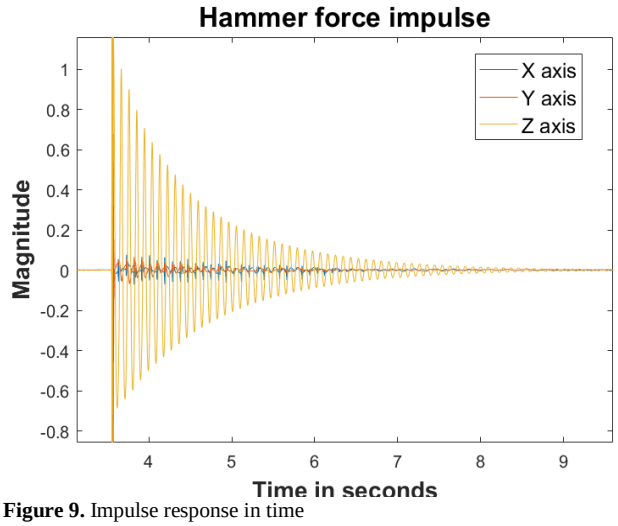

Figure 9. Impulse response in time

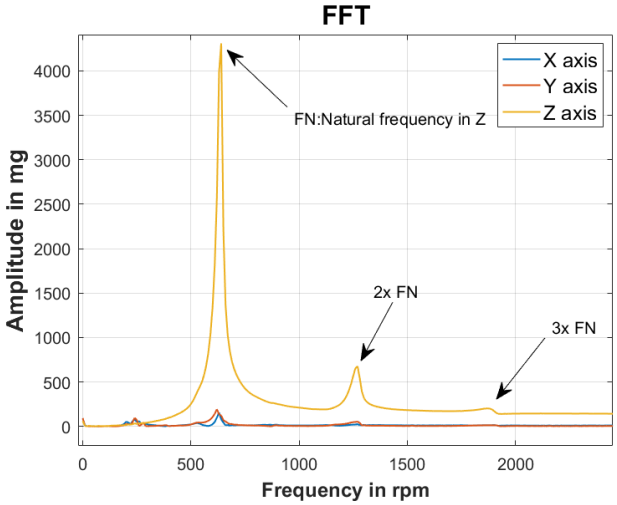

Figure 10. FFT to find the natural frequency of each axis

After all the tests performed, the data were extracted and separated by temperature and type of test as mentioned previously (type a, b, c and d). These results for the natural frequency of the Z axis are presented in the following table.

Table 2. Diferent tests and natural frequency ω_0 of Z axis in rad/s

	T=55K	T=65K	T=75K
Type a	66,93	66,58	67,16
Type b	61,52	61,80	61,94
Type c	68,55	69,60	72,21
Type d	62,39	63,49	64,58

With the values of the natural frequency of the harmonic system and oscillating masses it is possible through equation (2) to find the stiffness K. Using the values of the natural frequencies of table 2, the values of stiffness K are presented in table 3.

Table 3. Stiffness K [kN/m] value at each temperature

	T=55K	T=65K	T=75K
Type a	5,30	5,24	5,34
Type b	14,77	14,91	14,97
Type c	5,56	5,73	6,17
Type d	15,19	15,74	16,28

It is possible to observe that in the tests without flux pump (a and b) the values of K have insignificant variation with the temperature. And in the tests in which the flux pump (c and d) was performed, there is greater dependence on temperature.

By analyzing equation (3), it is clear that the damping factor $\boldsymbol{\xi}$ can be used to calculate the damping constant c. For this, the logarithmic decrement δ will be used.

$$\boldsymbol{\delta = \frac{1}{n}\ln\left(\frac{A}{A_n}\right)} \quad (4)$$

$$\boldsymbol{\delta = \frac{2\pi\xi}{\sqrt{1-\xi^2}}} \quad (5)$$

$$\boldsymbol{\xi = \sqrt{\frac{\delta^2}{4\pi^2+\delta^2}}} \quad (6)$$

Through a small manipulation, it is possible to show that equation (5) can be rewritten as equation (6) in which the damping factor $\boldsymbol{\xi}$ becomes evident and it is possible to calculate it using the logarithmic decrement δ.

It is also known that:

$$\boldsymbol{C_c = 2m_{eq}\omega_0} \quad (7)$$

$$\boldsymbol{\xi = \frac{C}{C_c}} \quad (8)$$

In equation 4, n is the number of peaks observed, and A is the amplitude of the first peak, A_n is the amplitude of the nth peak.

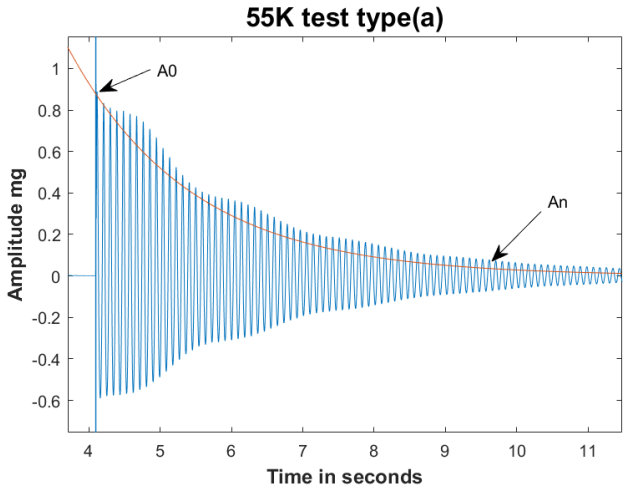

Figure 11. Logarithmic decrement behavior

After processing the data using equations (4 to 8), it is possible to set up a table with the dynamic data of the system damping separated by temperature and by type of test. These tables can be viewed below.

Table 4. Damping data for the tests with temperature equal to **55K**

Type (a)		Type (b)	Type (c)	Type (d)
A_0	0,8886	0,4662	1,542	0,6892
A_N	0,1059	0,11	0,2932	0,2431
n	50	50	35	26
δ	0,04254	0,02888	0,04743	0,04008
ξ	0,00677	0,00460	0,00755	0,00638
m_{eq}	1,18	3,9	1,18	3,9
ω_0	66,93	61,52	68,55	62,39
ω_d	66,93	61,52	68,55	62,39
c_c	157,95	479,86	161,78	486,64
c	1,07	2,21	1,22	3,10

Table 5 Damping data for the tests with temperature equal to **65K**

Type (a)		Type (b)	Type (c)	Type (d)
A_0	1,074	0,4719	0,412	1,646
A_N	0,1261	0,03709	0,02968	0,08869
n	23	30	30	30
δ	0,09313	0,08478	0,08768	0,09737
ξ	0,01482	0,01349	0,01395	0,01549
m_{eq}	1,18	3,9	1,18	3,9
ω_0	66,58	61,8	69,6	63,49
ω_d	66,57	61,79	69,59	63,48
c_c	157,13	482,04	164,26	495,22
c	2,33	6,50	2,29	7,67

Table 6 Damping data for the tests with temperature equal to **75K**

Type (a)		Type (b)	Type (c)	Type (d)
A_0	1,278	0,5079	0,5652	1,382
A_N	0,06138	0,1668	0,1645	0,3599
n	30	30	30	25
δ	0,10120	0,03712	0,04114	0,05382
ξ	0,01610	0,00591	0,00655	0,00857
m_{eq}	1,18	3,9	1,18	3,9
ω_0	67,16	61,94	72,21	64,58
ω_d	67,15	61,94	72,21	64,58
c_c	158,50	483,13	170,42	503,72
c	2,55	2,85	1,12	4,31

Where C_c is the critical damping constant and c is the damping constant both in kg.s/m.

It is possible to note that all ξ <<1 and so the system is under damped. This explains why $\omega_d \approx \omega_0$.

The levitation heights were also measured and it is possible to plot the height versus stiffness graphs for each temperature test.

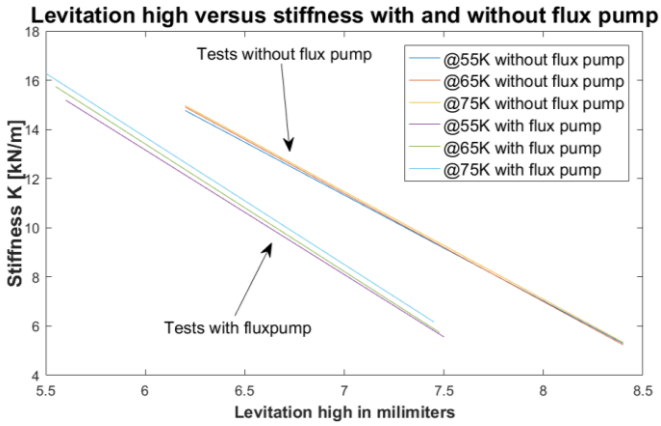

Figure 12. The diference between the stiffness with flux pump

Rotation tests were performed only with the disk mass. The resonance band was the same as the hammer experiment, thus confirming the obtained data.

IV. CONCLUSION

With the results of these experiments it was possible to observe that temperature does not influence in a significant way the dynamical behavior of the system. There is no evidence of benefit in reducing the temperature for the damping or natural frequencies of the superconducting bearing. All three set of tests at cryogenic temperatures showed that the system is under damped. The great advantage observed in the use of cryocooler in relation to the tests carried out in the past using liquid

nitrogen was the slow decay of the disk rotation since there is no more nitrogen vapor to generate drag in the rotor.

Acknowledgments

This development has been partially supported by the Brazilian agencies CNPq and FAPERJ and with the support of the Vibration Analysis Laboratory (LAVI) of UFRJ through the loan of its accelerometers and acquisition hardware.

References

[1] Z. Yu, G. Zhang, Q. Qiu, L. Hu, B. Zhuang, M. Qiu, "Analyses and Tests of HTS Bearing For Flywheel Energy System", *IEEE Transactions on Applied Superconductivity*, Vol. 24 (3), pp.1-5 2014.

[2] K. Murakami, M. Komori, H. Mitsuda, A. Inoue, , "Design of an energy storage flywheel system using permanent magnet bearing (PMB) and superconducting magnetic bearing (SMB)", *Cryogenics*, vol. 47 (4), pp. 272277, 2007.

[3] Y. Arai, H. Seino, K. Yoshizawa, K. Nagashima, "Development of superconducting magnetic bearing with superconducting coil and bulk superconductor for flywheel energy storage system", *Physica C: Superconductivity and its applications*, Vol.494, pp.250-254 2013.

[4] M H Ali, B Wu and R A Dougal "An overview of smesapplications in power and energy systems", *IEEE Trans. Sustainable Energy*, 1 38–47 2010.

[5] F N Werfel, U Floegel-Delor, R Rothfeld, T Riedel, B Goebel, D Wippich and P Schirrmeister, "Superconductorbearings, flywheels and transportation", *Supercond. Sci. Technol*. 25 014007 2012.

[6] S. Celik, "Design of magnetic levitation force measurement system at any low temperatures from 20K to room temperature", *Journal of Alloys and Compounds*, Pages 546-556, 2016

[7] B. Zheng, J. Zheng, D. He, Y. Ren, Z. Deng, "Magnetic characteristics of permanent magnet guideways at low temperature and its effect on the levitation force of bulk YBaCuO superconductors", Journal of Alloys and Compounds, Pages 77-81, 2016

[8] C. Chiang, C. Yang, P. Hsieh, W. Chan, "Levitation Force Measurement at Different Temperatures for YBCO Superconductor", *Journal of Low Temperature Physics*, pp.743-746, 2003.

[9] P. Bernstein, L. Colson, L. Dupont, J. Noudem, "Investigation of the levitation force of field-cooled YBCO and MgB2 disks as functions of temperature", *Superconductor Science and Technology*, Vol. 30 (6), p.065007 (8pp) 2017.

[10] A Sharma, V V Tyagi, C R Chen and D Buddhi, "Review on thermal energy storage with phase changematerials and applications", *Renew. Sustainable EnergyRev*. 13 318–45, 2009.

[11] R Saidur, N A Rahim and M Hasanuzzaman, "A review oncompressed-air energy use and energy savings", *Renew.Sustainable Energy*, Rev. 14 1135–53, 2010.

[12] G G Sotelo, D H N Dias, R Jr De Andrade and R M Stephan, "Tests on a superconductor linear magnetic bearing of a full-scale maglev vehicle", *IEEE Trans. Appl. Supercond*, 1464–8, 2011.

[13] G G Sotelo, A C Ferreira and R de Andrade, "Halbacharray superconducting magnetic bearing for a flywheelenergy storage system", *IEEE Trans. Appl. Supercond*., 152253–6 2005.

[14] G G Sotelo, R de Andrade and A C Ferreira, "Magnetic bearing sets for a flywheel system", *IEEE Trans. Appl. Supercond*., 17 2150–3, 2007.

[15] E Rodriguez, J de Santiago, J J Pérez-Loya, F S Costa, G G Sotelo, J G de Oliveira and R M Stephan, "Analysis of passive magnetic bearings for kinetic energy storage systems", *14th Int. Symp. on Magnetic*

[16] E Rodriguez, J J Pérez-Loya, J de Santiago, F S Costa, G G Sotelo, J G Oliveira and R M Stephan, "Passive magnetic bearing system", *22nd Int. Conf. on Magnetically Levitaded Systems and Linear Drives*, (Rio de Janeiro,Brazil) pp 1–9, 2014.

[17] G G Sotelo, E Rodriguez, F S Costa, J G Oliveira, J de Santiago and R M Stephan,' Tests with a hybrid bearing for a flywheel energy storage system', Supercond. Sci. Technol. 29 (2016) 095016 (10pp).

[18] Bo Wang , Jun Zheng, Shuaishuai Si, Nan Qian, Haitao Li , Jipeng Li , Zigang Deng," Dynamic response characteristics of the high-temperature superconducting maglev system under lateral eccentric distance", Elsevier Cryogenics 77 (2016) 1–7.

[19] R.M. Stephan , R. de Andrade Jr., G.C. dos Santos, M.A. Neves, R. Nicolsky,' Levitation force and stability of superconducting linear bearings using NdFeB and ferrite magnets', Physica C 386 (2003) 490–494

[20] E. Yanmaza,, K. Ozturka, C.E.J. Dancerc, M. Basoglua, S. Celikb, C.R.M. Grovenorc,' Levitation force at different temperatures and superconducting properties of nano-structured MgB2 superconductors', Journal of Alloys and Compounds 492 (2010) 48–51

[21] De Andrade R, Sotelo G G, Ferreira A C, Rolim L G B, da Silva Neto J L, Stephan R M, Suemitsu W I and Nicolsky R ,' Flywheel energy storage system description and tests', IEEE Trans. Appl. Supercond. 17 2154–7

[22] Murakami K, Komori M, Mitsuda H and Inoue A ,' Design of an energy storage flywheel system using permanent magnet bearing (PMB) and superconducting magnetic bearing (SMB)', 2007Cryogenics 47 272–7